



This discussion paper is/has been under review for the journal Atmospheric Chemistry and Physics (ACP). Please refer to the corresponding final paper in ACP if available.

Estimates of tropical bromoform emissions using an inversion method

M. J. Ashfold¹, N. R. P. Harris¹, A. J. Manning², A. D. Robinson¹, N. J. Warwick^{1,3},
and J. A. Pyle^{1,3}

¹Department of Chemistry, University of Cambridge, Cambridge, UK

²Met Office, Exeter, UK

³National Centre for Atmospheric Science, UK

Received: 20 July 2013 – Accepted: 24 July 2013 – Published: 6 August 2013

Correspondence to: M. J. Ashfold (mja63@cam.ac.uk)

Published by Copernicus Publications on behalf of the European Geosciences Union.

Estimates of tropical bromoform emissions using an inversion method

M. J. Ashfold et al.

Title Page

Abstract

Introduction

Conclusions

References

Tables

Figures

⏪

⏩

◀

▶

Back

Close

Full Screen / Esc

Printer-friendly Version

Interactive Discussion

Abstract

Bromine plays an important role in ozone chemistry in both the troposphere and stratosphere. When measured by mass, bromoform (CHBr_3) is thought to be the largest organic source of bromine to the atmosphere. While seaweed and phytoplankton are known to be dominant sources, the size and the geographical distribution of CHBr_3 emissions remains uncertain. Particularly little is known about emissions from the Maritime Continent, which have usually been assumed to be large, and which appear to be especially likely to reach the stratosphere. In this study we aim to use the first multi-annual set of CHBr_3 measurements from this region, and an inversion method, to reduce this uncertainty. We find that local measurements of a short-lived gas like CHBr_3 can only be used to constrain emissions from a relatively small, sub-regional domain. We then obtain detailed estimates of both the distribution and magnitude of CHBr_3 emissions within this area. Our estimates appear to be relatively insensitive to the assumptions inherent in the inversion process. We extrapolate this information to produce estimated emissions for the entire tropics (defined as 20°S – 20°N) of $225\text{ Gg CHBr}_3\text{ yr}^{-1}$. This estimate is consistent with other recent studies, and suggests that CHBr_3 emissions in the coastline-rich Maritime Continent may not be stronger than emissions in other parts of the tropics.

1 Introduction

Chemical cycles involving inorganic bromine species (Br_y) are known to destroy appreciable quantities of ozone (O_3) in both the stratosphere (e.g. Salawitch et al., 2005) and troposphere (Yang et al., 2005; Read et al., 2008; Parrella et al., 2012). The largest source of Br_y , by mass, appears to be release from sea-salt aerosols in the marine boundary layer (Ayers et al., 1999; Yang et al., 2005; Parrella et al., 2012). The lifetime of Br_y in the lower troposphere is short enough that this direct inorganic source does not appear to significantly influence chemistry at higher altitudes (e.g. Yang et al.,

ACPD

13, 20463–20502, 2013

Estimates of tropical bromoform emissions using an inversion method

M. J. Ashfold et al.

Title Page

Abstract

Introduction

Conclusions

References

Tables

Figures

◀

▶

◀

▶

Back

Close

Full Screen / Esc

Printer-friendly Version

Interactive Discussion

Estimates of tropical bromoform emissions using an inversion method

M. J. Ashfold et al.

Title Page

Abstract

Introduction

Conclusions

References

Tables

Figures

⏪

⏩

◀

▶

Back

Close

Full Screen / Esc

Printer-friendly Version

Interactive Discussion

2005). In contrast, a class of man-made organic bromine compounds, the halons, provide a significant source of Br_y to the stratosphere (e.g. Wamsley et al., 1998). There are also naturally occurring organic bromine compounds, which are known to be emitted by seaweed (e.g. Gschwend et al., 1985; Manley et al., 1992; Itoh and Shinya, 1994) and phytoplankton (e.g. Sturges et al., 1992; Tokarczyk and Moore, 1994; Moore et al., 1996). These compounds have shorter atmospheric lifetimes than their man-made counterparts, typically of weeks to months, and are often referred to as very short-lived substances (VSLs). They may be the dominant source of Br_y in the upper troposphere and lowermost stratosphere (Dvortsov et al., 1999; Salawitch et al., 2005). Bromoform (CHBr_3) and dibromomethane (CH_2Br_2) have received most attention, and appear to account for the bulk of bromine bound within VSLs (Hossaini et al., 2012). A further organic source of bromine is methyl bromide (CH_3Br), which has an intermediate lifetime of ~ 1 yr and a more diverse range of both natural and man-made sources (Saltzman et al., 2004). Overall, these sources combine to give a present stratospheric Br_y loading of 22.5 (19.5–24.5) ppt (Montzka and Reimann, 2011).

Anthropogenic organic bromine emissions, and associated global average mixing ratios, are thought to be reasonably well quantified (Montzka and Reimann, 2011). Conversely, there remains much uncertainty in our understanding of the magnitude and distribution of the predominantly natural emissions of VSLs. Broadly, two main methods have been used to arrive at estimates of global CHBr_3 fluxes. In the “bottom-up” method local flux calculations are assumed to be representative of, and are extrapolated over, particular oceanic domains (e.g. Quack and Wallace, 2003; Carpenter and Liss, 2000; Butler et al., 2007; Ziska et al., 2013). In the “top-down” method an idealised pattern of emissions is typically assumed based on available observational evidence and the emission magnitude is then varied to match observations made in the “background” atmosphere (e.g. Warwick et al., 2006; Liang et al., 2010; Ordóñez et al., 2012). In addition, observations of compounds with a common source but different lifetimes can be used to derive emission estimates (e.g. Yokouchi et al., 2005), and parameterisations of emissions based on physical and biological variables have begun to be considered

Estimates of tropical bromoform emissions using an inversion method

M. J. Ashfold et al.

Title Page

Abstract

Introduction

Conclusions

References

Tables

Figures

⏪

⏩

◀

▶

Back

Close

Full Screen / Esc

Printer-friendly Version

Interactive Discussion

(Palmer and Reason, 2009). Estimates of CHBr_3 emissions are made difficult by its short lifetime (as low as 2 weeks in the tropics, e.g. Warwick et al., 2006; Hossaini et al., 2010), which ensures that measured mixing ratios are often highly variable, and are likely to be influenced by only a small fraction of global sources. For comparison, recent global emission estimates of the longer-lived CH_2Br_2 (which has a lifetime of months, e.g. Warwick et al., 2006; Hossaini et al., 2010) have converged on a value of $\sim 60 \text{ Gg yr}^{-1}$ (e.g. Liang et al., 2010; Ordóñez et al., 2012). One part of the world where CHBr_3 emissions are particularly poorly constrained is the Maritime Continent, where long-term observations have only recently become available (e.g. Pyle et al., 2011; Robinson et al., 2013). The Maritime Continent is important because a number of studies have suggested that emissions from this convectively active region may be much more likely to contribute to stratospheric Br_y (e.g. Levine et al., 2007; Aschmann et al., 2009; Hosking et al., 2010; Pisso et al., 2010).

In this study we attempt to improve our understanding of CHBr_3 emissions in the Maritime Continent. To do this we use the first long-term set of observations collected in this region (described by Robinson et al., 2013) and an inversion method (Manning et al., 2003, 2011), which has been used to estimate emissions of long-lived greenhouse gases and ozone-depleting substances (see also O'Doherty et al., 2004; Reimann et al., 2005; Polson et al., 2011). This work, focussed on measurements of a short-lived compound in the deep tropics, represents a new application of this method. We therefore aim to consider the limitations and additional uncertainties associated with the choice of this type of modelling tool for our particular purpose. The paper is structured as follows: in Sect. 2 we introduce the observations we use to constrain our model; in Sect. 3 we provide details of the modelling tools we employ; in Sect. 4 we show that our method can successfully locate a “known” emission distribution; in Sect. 5 we present our estimates of CHBr_3 emissions in the Maritime Continent; and finally, in Sect. 6, we compare our estimate with previous work, we discuss the limitations of our method, and we recommend ways this type of study can be improved in the future.

2 Bromoform observations

We use CHBr_3 observations which are presented in detail by Robinson et al. (2013). The main features are summarised again here. The measurements were collected using University of Cambridge μ -Dirac instruments (Gostlow et al., 2010) at two locations in Sabah, Malaysia, and cover the period April 2008–May 2010. One instrument was located ~ 50 km from the nearest coast, at the Bukit Atur Global Atmospheric Watch site, within the Danum Valley Conservation Area. The second instrument was located at the coast, near the town of Tawau, and ~ 85 km south of Bukit Atur. The characteristics of the two measurement locations, and the quality of our data, are discussed by Robinson et al. (2013). Figure 1 shows the CHBr_3 measurements, which have been averaged over 3 h intervals to allow direct comparison with our model calculations (see Sect. 3). The sampling rate of μ -Dirac means there are typically ~ 6 measurements in these 3 h windows. We will refer to these averaged data simply as “observations”. Our CHBr_3 observations are a major enhancement to the quantity of information available in the Maritime Continent, as until recently measurements have been collected only during occasional cruises through the region (e.g. Quack and Suess, 1999; Yokouchi et al., 1999).

The CHBr_3 mixing ratio at Tawau, on the coast, is occasionally many tens of ppt, and above 3.51 ppt (the red line in Fig. 1) in 10 % of the observations. Additional quantitative information can be found in the probability density functions, PDFs, presented by Robinson et al. (2013). While Robinson et al. (2013) do not identify a specific local cause of these high mixing ratios, previous studies have typically found such levels of CHBr_3 when seaweed are nearby (e.g. Carpenter and Liss, 2000; Pyle et al., 2011). Aside from these periods, mixing ratios at Tawau are usually within the range 1–2 ppt. While there is often a small gradient in background mixing ratio between the coast and inland (again refer to the PDFs in Robinson et al., 2013), the majority of our inland data, and indeed many other observations apparently made away from strong CHBr_3 sources (see Table 1–7 of Montzka and Reimann, 2011), also lie within this range.

Estimates of tropical bromoform emissions using an inversion method

M. J. Ashfold et al.

Title Page

Abstract

Introduction

Conclusions

References

Tables

Figures



Back

Close

Full Screen / Esc

Printer-friendly Version

Interactive Discussion

Estimates of tropical bromoform emissions using an inversion method

M. J. Ashfold et al.

Title Page

Abstract

Introduction

Conclusions

References

Tables

Figures

⏪

⏩

◀

▶

Back

Close

Full Screen / Esc

Printer-friendly Version

Interactive Discussion

Our data are used here to inform an inversion process, and so it is important to consider how observational uncertainties might impact our estimates of CHBr_3 emissions. First, calibration errors might lead to biases in our observations, and in our subsequent emission estimates. A recent measurement inter-comparison (Jones et al., 2011) suggests that for CHBr_3 , discrepancies of ~ 10 – 20% are possible. As this uncertainty is likely to manifest itself as a bias, we attempt to assess its potential significance by repeating our inversion calculations with a range of “baseline” mixing ratios (see Sect. 3.2.2).

Another metric for measurement uncertainty is the precision, which we define as the standard deviation of calibration peak heights divided by the mean height of such peaks (see also Robinson et al., 2013). Though the measurement precision varied throughout the period covered, and was not identical at the two locations, we use 7% (i.e. 0.14 ppt, where the multi-site mean mixing ratio is 1.96 ppt) as a value representative of this type of uncertainty. The measurement precision uncertainty is likely to be smaller than the uncertainty attached to the model calculations (Sect. 3.1) and to the assumptions inherent in the inversion method (Sect. 3.2), and is therefore incorporated into an overall uncertainty which is implemented as “noise” within the inversion process (see Sect. 3.2.4).

3 Modelling tools

In this section we first describe the atmospheric transport model we have used to calculate the immediate history of the air masses measured in Borneo. Section 3.2 introduces the associated inversion method used to estimate CHBr_3 emissions, and discusses the assumptions and approximations this method requires.

3.1 NAME trajectory calculations

To interpret our measurements we have used the UK Met Office's Lagrangian atmospheric dispersion model, NAME (Jones et al., 2007). NAME allows the calculation of trajectories using three-dimensional meteorological fields, which are produced by the UK Met Office's Unified Model (UM) during operational weather forecasts, and are available at 3 hourly intervals. For most of our observational period they have a horizontal resolution of 0.5625° longitude by 0.375° latitude, though this was improved to $\sim 0.35^\circ$ by $\sim 0.23^\circ$ in February 2010. Within NAME a parameterisation of turbulence is also used (see Webster et al., 2003; Morrison and Webster, 2005).

NAME was used to calculate batches of 33 000 backward trajectories, released at random throughout each 3 h period for which CHBr_3 measurements were available at a particular location. In our measurement window there were a total of 2350 such periods at Bukit Atur, and 2726 at Tawau (see also Fig. 1). The trajectories were started randomly within an altitude range of 0–100 m. They ran for 12 days, and every 15 min the location of all trajectories within the lowest 100 m of the model atmosphere was recorded on a grid with the same resolution as the driving meteorological fields (always 0.5625° by 0.375°). By counting only the “near-surface” trajectories a picture was built up of the areas from which surface emissions could have influenced the measured air masses during the previous 12 days. Quantitatively, these trajectories contribute to a “dilution matrix” (units of s m^{-1}) which, for each 3 h period, gives the multiplicative factor by which emissions in a particular grid cell are diluted by the time they have travelled to a measurement location (see Manning et al., 2011). We attempt to account for the effect of photochemical loss of CHBr_3 by assigning each trajectory a mass that decays with an e-folding time of 15 days (an approximation to the expected lifetime of CHBr_3 in the tropical lower troposphere, Warwick et al., 2006; Hossaini et al., 2010; Liang et al., 2010). This has the effect of decreasing the dilution value in grid cells further from the measurement locations.

Estimates of tropical bromoform emissions using an inversion method

M. J. Ashfold et al.

Title Page

Abstract

Introduction

Conclusions

References

Tables

Figures

⏪

⏩

◀

▶

Back

Close

Full Screen / Esc

Printer-friendly Version

Interactive Discussion



Estimates of tropical bromoform emissions using an inversion method

M. J. Ashfold et al.

Title Page

Abstract

Introduction

Conclusions

References

Tables

Figures



Back

Close

Full Screen / Esc

Printer-friendly Version

Interactive Discussion



Figure 2 shows the time-averaged dilution matrix, calculated over all 3 h periods for which observations are available at either location. It shows that the sites in Borneo are influenced by two prevailing wind directions, with northeasterly trade winds dominating during Northern Hemisphere winter, and southeasterlies during Northern Hemisphere summer. It also shows that large fractions of the plotted domain are crossed by relatively few trajectories (dilution values range over six orders of magnitude), and emissions in these regions are unlikely to appreciably affect our measurements. One implication, which is typical of the inversion method we employ, and is discussed next in Sect. 3.2.1, is that our emission estimates are made on a non-uniform grid, with larger grid cells used where there is less dilution information.

Our emission estimates will be affected by any errors in the meteorological data used to drive NAME, and in the dispersion calculations within NAME. The estimates of Manning et al. (2011) were relatively insensitive to the choice of meteorology, though their study was focussed on mid-latitudes. In the tropics, the representation of convection will be more important, and will be necessarily incomplete in any set of meteorological analyses. In addition, the local meteorology at both Bukit Atur, where changes in boundary layer height appear to be critical to determining atmospheric composition (e.g. Pike et al., 2010), and Tawau, where a “sea breeze” circulation is common (Qian et al., 2013), may not be represented accurately in a global model such as the UM. Finally, the rate at which air masses (i.e. trajectories) are mixed between the boundary layer and free troposphere in NAME will have a significant impact on our estimated emissions. Pyle et al. (2011) showed, and we reiterate in Sect. 4, that in the Maritime Continent this type of mixing seems to be weaker in NAME than in another model, p-TOMCAT. We attempt to assess the possible impact of these model-related uncertainties both by adding “noise” to our inversion process, and by adjusting the “baseline” CHBr_3 mixing ratio (see Sect. 3.2.4).

3.2 Inversion method

The inversion method employed here has been described by Manning et al. (2003, 2011), and can be summarised by Eq. (1). Using an optimisation process, the aim is to locate the emission map, that can be multiplied by a NAME dilution matrix, to give modelled concentrations at a measurement site that most closely resemble the observed concentrations (converted from volume mixing ratios using UM meteorological data).

$$\text{emission (g m}^{-2} \text{ s}^{-1}) \times \text{dilution (s m}^{-1}) = \text{concentration (g m}^{-3}) \quad (1)$$

Importantly, in this method emissions are assumed to be constant in time; clearly, when considering a compound with large natural emissions such as CHBr_3 , this is likely to be a source of error in our estimates. In this section we discuss some of the other assumptions that are implicit in the method, which has typically been used to estimate emissions of compounds with lifetimes of years. So we also aim to highlight further uncertainties that are peculiar to our compound of interest, CHBr_3 , with its much shorter lifetime.

3.2.1 The solution grid

The dilution matrix in Fig. 2 shows that air is most likely to travel towards our measurement locations from either the southeast or northeast, and more likely to travel over grid cells near to a measurement location than those further away. It is difficult to assess how the observations will be affected by emissions from a particular grid cell if air seldom passes over it. Such grid cells are therefore grouped together using the method of Manning et al. (2011), into progressively larger squares of 2 by 2 cells, 4 by 4 cells and so on. As a result, the contribution to the observations from emissions in the new, grouped grid cell is larger or more frequent. This solution grid, containing grouped cells, is shown in Fig. 3, and is used for each of the inversion experiments in this study. We tested changing the resolution of the solution grid but found that such changes had a small impact on the results we present in Sect. 5.

20471

ACPD

13, 20463–20502, 2013

Estimates of tropical bromoform emissions using an inversion method

M. J. Ashfold et al.

Title Page

Abstract

Introduction

Conclusions

References

Tables

Figures

⏪

⏩

◀

▶

Back

Close

Full Screen / Esc

Printer-friendly Version

Interactive Discussion



Estimates of tropical bromoform emissions using an inversion method

M. J. Ashfold et al.

Title Page

Abstract

Introduction

Conclusions

References

Tables

Figures

⏪

⏩

◀

▶

Back

Close

Full Screen / Esc

Printer-friendly Version

Interactive Discussion

We can use the dilution matrix (Fig. 2) to assess the influence that emissions in solution grid cells of particular sizes might have on our measurements. If we assume that a tracer is emitted uniformly across our region of interest the dilution matrix can be used to derive a modelled concentration (Eq. 1). Figure 4 shows the cumulative contribution to this modelled concentration when the individual dilution grid cells in Fig. 2 are added in turn (beginning with the largest dilution value). The red line (and label) shows that 44 % of this modelled concentration is due to emissions in solution grid cells of size 1 by 1, and that these cells cover an area of $1.65 \times 10^{11} \text{ m}^2$ ($\sim 0.1 \%$ of the tropics, see Table 1). The orange (2 by 2), blue (4 by 4) and grey (8 by 8 to 32 by 32) lines indicate this relationship when solution grid cells of increasing size are also included in the calculation.

Throughout the rest of the paper we will focus on emissions in the smaller grid cells, of size 1 by 1 and 2 by 2 only (coloured in red and orange in Fig. 3). We refer to these as “fine” grid cells. We make this choice because they are the grid cells for which most dilution information is available, and from which emissions are likely to have the greatest impact on the observations. Conversely, emissions from the coarser solution grid cells can vary significantly while having only a small impact on the observations, and will therefore be less reliably constrained by the inversion method. Figure 4 shows that the “fine” cells account for almost two thirds of the observed signal from a uniform emission across our solution grid, while accounting for only $\sim 3 \%$ of the area. This demonstrates that the compromise between considering emissions for which there is reasonable dilution information, and estimating emissions over a usefully-sized area, is a delicate one. We have repeated our analyses using only the 1 by 1 cells, and using all cells up to size 4 by 4 (the areas covered by these different grids are given in Table 1), and will occasionally refer to these results. Overall though, we find that our choice of “fine” grid does not significantly affect our conclusions.

3.2.2 The “baseline”

Our backward trajectories can only be used to account for emissions occurring within the last 12 days. The contribution from earlier emissions therefore needs to be estimated, and subtracted from the observations. In the case of long-lived gases like CFCs, well-defined “baseline” mixing ratios can be observed at remote, unpolluted locations. Subtracting the baseline mixing ratio from such observations should therefore leave only pollution episodes caused by recent emissions. Here, though, where the compound of interest is short-lived, the concept of a baseline is less applicable. In addition, and in contrast to gases such as CFCs which have geographically discrete sources, CHBr₃ is thought to be emitted over much of the ocean (e.g. Butler et al., 2007). Therefore, in the Maritime Continent, air masses travelling in any direction towards the measurement locations may be subject to CHBr₃ emissions. With a lifetime of ~ 15 days though, it is also likely there is some contribution to the CHBr₃ observations from emissions that occur more than 12 days previously, and that are therefore outside our solution grid.

In our experiments we use a constant baseline. This is a simplification, but there is no clear reason to select particular air masses that might enable the construction of a time-varying baseline. In addition, our results are similar if a seasonally varying baseline is employed (not shown). In the majority of the inversions we use a baseline mixing ratio of 0.43 ppt. This is the mean contribution from “rest of world” sources (i.e. those outside of a Southeast Asian domain of similar size and location to our solution grid) to the modelled CHBr₃ mixing ratio at Bukit Atur in a multi-year p-TOMCAT simulation containing Pyle et al. (2011) emissions. Our choice of baseline mixing ratio is also close to the minimum observed value (0.40 ppt, see Fig. 1) so is consistent with an alternative definition based on the CHBr₃ measurements. To examine how sensitive our emission estimates are to this choice, we conduct additional experiments in which the baseline is shifted up/down by one standard deviation of the p-TOMCAT “rest of world” contribution to Bukit Atur (± 0.19 ppt). These additional experiments also allow

Estimates of tropical bromoform emissions using an inversion method

M. J. Ashfold et al.

Title Page

Abstract

Introduction

Conclusions

References

Tables

Figures



Back

Close

Full Screen / Esc

Printer-friendly Version

Interactive Discussion



us to indirectly assess the possible impact of biases (e.g. in measurement calibration, or in the rate of modelled boundary layer to free troposphere mixing) on our estimated emissions.

3.2.3 Optimisation

The aim of the optimisation process, which is outlined in this section, is to find the emission distribution that provides the “best” match between the modelled time series and the observed time series. We use the normalised mean square error (NMSE, Eq. 2) as a cost function to judge the strength of the agreement between model (m) and observation (o), and it is this error that the optimisation process will seek to minimise.

$$\text{NMSE} = \frac{1}{n} \sum_{i=1}^n \frac{(m_i - o_i)^2}{\bar{m}\bar{o}} \quad (2)$$

Our cost function could have many configurations, so we acknowledge that this choice may be a source of uncertainty. However, we obtain similar results if we use either the root mean square error or a cost function similar to that employed by Manning et al. (2011) with a mix of statistical measures.

If something is thought to be known about an emission distribution (for example, Stohl et al., 2009, assume zero oceanic emissions of selected anthropogenic halocarbons) then this knowledge can be incorporated into the cost function. Again, the weighting (equivalently the confidence) assigned to this so-called a priori information is subjective. As Manning et al. (2011) aim to generate an emission estimate that is entirely independent of “bottom-up” inventories, they do not use any a priori information. We believe that the characteristics of CHBr₃ emissions are not known sufficiently well to warrant the use of a prior, with the exception that there is little evidence for terrestrial sources. As such, rather than altering the cost function, our sole use of a priori information is to fix land emissions to be zero in some of our experiments.

Estimates of tropical bromoform emissions using an inversion method

M. J. Ashfold et al.

Title Page

Abstract

Introduction

Conclusions

References

Tables

Figures

⏪

⏩

◀

▶

Back

Close

Full Screen / Esc

Printer-friendly Version

Interactive Discussion

The optimisation method used to minimise the cost function is “simulated annealing”, so-called because of its conceptual similarity to annealing in metallurgy. The method is described in detail by both Kirkpatrick et al. (1983) and Press et al. (1986), and its application here is described by Manning et al. (2011). This particular approach is useful when, as is the case here, there are so many possible solutions to a problem that an exhaustive search for the optimum solution (i.e. the minimum cost) is impractical. The method therefore aims to find a solution that can not be improved upon significantly while using only limited computing time. We repeat each inversion experiment 25 times to obtain a range of emission estimates, with different solutions emerging due both to noise added to the observations (Sect. 3.2.4) and to random changes made during the iterative optimisation procedure.

3.2.4 “Noise” and uncertainty

As suggested in Sect. 2, there is a range of sources of uncertainty in the emission estimates based on Eq. (1). While we are able to quantify the uncertainty related to measurement precision with reasonable confidence (Sect. 2), the uncertainty attached to the model calculations and to the assumptions inherent in the inversion method is more difficult to ascertain (see also Manning, 2011). In an attempt to account for these uncertainties a time series of “noise” (selected at random from a normal distribution with a mean of zero, and with a specified standard deviation) is added to the observations (or equivalently, to the baseline which is subtracted from the observations, see Fig. 1). As noted in the preceding section, the inversion process is repeated 25 times, with the aim of each inversion attempt to find emissions that best match a different randomly altered set of observations.

For the inversion experiments presented in Sect. 5 we use a standard deviation of ± 0.24 ppt for the normally distributed random numbers we add to the observations. This is the sum of two normal distributions: the first, with a standard deviation of 0.14 ppt, represents measurement precision uncertainty (see Sect. 2), and the second, with a standard deviation of 0.19 ppt, represents baseline uncertainty (Sect. 3.2.2). We have

the known oceanic sources of CHBr_3 . However, emissions from coastal grid cells are relatively small (16 %); as seaweed are thought to be a major CHBr_3 source in this region (Pyle et al., 2011) this finding is perhaps unexpected.

Of course, the observations collected at Bukit Atur and Tawau are not independent of one another; they are the result of the same distribution of CHBr_3 emissions. So in experiment B the observations from both sites are used in the same inversion. The total emission from the “fine” solution grid cells increases by $\sim 70\%$ to 2.2 (2.0–2.3 Gg $\text{CHBr}_3 \text{ yr}^{-1}$) when we include these coastal data with, on average, higher mixing ratios. The distribution of emissions is also somewhat different, with a larger percentage of emissions found both along coastlines (26 %, again see Table 2), which, given known CHBr_3 sources, we might expect, and inland areas (23 %), which we might not. The statistical agreement between the observations and the modelled concentration is weaker (NMSE = 1.05) than in experiment A. This difference is largely caused by the occasional very high mixing ratios at the coast, which are presumably strongly influenced by emissions occurring very close to the Tawau site. These emissions will not be diluted according to the local value of the dilution matrix, and will therefore be difficult for the inversion method to account for.

In experiment C we attempt to remove the impact of these very local emissions. This is done by capping the coastal observations at the 90th percentile (3.51 ppt, marked with a red line in Fig. 1). All higher mixing ratios are set to this threshold. We accept that this is a crude approximation, but in support of our choice, we note that the 90th percentile of the coastal observations is very similar to the 99th percentile mixing ratio observed inland at Bukit Atur (3.55 ppt), where we assume there are no local sources. We also repeated this experiment using the 80th (2.65 ppt) and 95th (4.75 ppt) percentiles as our threshold and found only small ($\sim 10\%$) differences in the total estimated emission magnitude. The total emission from the “fine” grid cells is now 1.4 (1.3–1.5) Gg $\text{CHBr}_3 \text{ yr}^{-1}$; slightly higher than in experiment A, but lower than experiment B where the full range of coastal observations was included. Similarly, the distribution of emissions lies between experiments A and B, with 17 % from land, 21 % from coastal

Estimates of tropical bromoform emissions using an inversion method

M. J. Ashfold et al.

Title Page

Abstract

Introduction

Conclusions

References

Tables

Figures

⏪

⏩

◀

▶

Back

Close

Full Screen / Esc

Printer-friendly Version

Interactive Discussion



grid cells and 62 % from the ocean (Table 2). The statistical agreement is almost as strong as in experiment A (NMSE = 0.26), confirming that the highest CHBr_3 mixing ratios at the coast lead to the poorer statistical agreement in experiment B.

In experiment D we repeat experiment C, but enforce an a priori condition of zero emissions from solution grid cells that contain only land. The inversion process remains free to attribute emissions to grid cells containing a mix of land and ocean. As CHBr_3 emissions are thought to be dominated by oceanic sources it is encouraging that, according to our cost function, the solutions to experiments C and D are of equal quality (NMSE = 0.26). Emissions from the “fine” solution grid cells total 1.3 (1.1–1.4) $\text{Gg CHBr}_3 \text{ yr}^{-1}$, a little lower than without the “no land” constraint, and are now mostly distributed between the coast (25 %) and ocean (67 %). The remaining land emissions are placed in solution grid cells which contain both land and ocean, and so in reality are likely to be coastal emissions. In a similar way, some of the emissions attributed to land in experiments A, B and C are likely, in reality, to be due to coastal sources.

The data in Table 3 allow us to examine the effect that our choice of “fine” grid cells has on the split between land, coast and ocean emissions in experiment D. Recall that in this experiment land emissions are fixed to zero where the solution grid is of sufficient resolution. The area-averaged CHBr_3 flux from these three surface types is similar when grid cells of size either 1 by 1 or 2 by 2 are the maximum allowed, which suggests that including the extra area of 2 by 2 grid cells is a useful step. In contrast when the maximum grid cell size is 4 by 4, a much larger fraction of emissions is attributed to land within the coarser parts of the grid.

In the final pair of experiments, we twice repeat experiment D with a different baseline mixing ratio. In experiment E the baseline is lower than our best estimate, at 0.24 ppt. In F it is higher, at 0.62 ppt. As noted at the end of Sect. 3.2.2, these experiments allow us to assess the possible impact of biases, such as calibration errors, on our estimated emissions. As might be expected, the total emission from the “fine” grid cells in experiment D falls between the total with a lower baseline, 1.5 (1.3–1.6) $\text{Gg CHBr}_3 \text{ yr}^{-1}$,

Estimates of tropical bromoform emissions using an inversion method

M. J. Ashfold et al.

Title Page

Abstract

Introduction

Conclusions

References

Tables

Figures



Back

Close

Full Screen / Esc

Printer-friendly Version

Interactive Discussion

within each grid cell was used to attribute emissions to each surface type. However, this new definition yielded similar results, and does not affect our conclusions.

6 Summary and discussion

In this study we have examined a new method to quantify CHBr_3 emissions. We use an inversion process, informed by new long-term observations from Borneo and NAME trajectory calculations, to investigate systematically the distribution and magnitude of CHBr_3 emissions in the Maritime Continent. We examine how sensitive the estimated CHBr_3 emissions are to the characteristics of our measurements, and to assumptions in the inversion methodology.

We find that our local measurements of a short-lived compound like CHBr_3 , with presumed diffuse sources, are overwhelmingly influenced by emissions from within a relatively small “footprint”, covering $< 1\%$ of the tropics (20°S – 20°N). This is also likely to be true of other CHBr_3 measurements, and means that observations from a very large number of sites would be required to obtain global coverage. Within the footprint region our results are robust, with the various sensitivities considered often leading to relatively minor changes, and emissions totalling 1.1 – $1.4\text{ Gg CHBr}_3\text{ yr}^{-1}$. Even without a priori constraint these emissions were largely distributed within oceanic grid cells, which is consistent with expected algal sources.

An extrapolation of the flux calculated in experiment D results in tropical (20°S – 20°N) emissions of $225\text{ Gg CHBr}_3\text{ yr}^{-1}$, with possible lower and upper bounds (180 and $280\text{ Gg CHBr}_3\text{ yr}^{-1}$) provided by varying the baseline mixing ratio in experiments E and F. Our estimate is comparable to those arrived at in recent global modelling studies. For the tropics defined as 20°S – 20°N , these emissions include $\sim 240\text{ Gg CHBr}_3\text{ yr}^{-1}$ (Liang et al., 2010), $\sim 310\text{ Gg CHBr}_3\text{ yr}^{-1}$ (Warwick et al., 2006, updated by Pyle et al. 2011) and $\sim 300\text{ Gg CHBr}_3\text{ yr}^{-1}$ (Ordóñez et al., 2012). Our estimate, however, is somewhat higher than the “bottom up” estimate of Ziska et al. (2013), who used two different statistical methods to arrive at a tropical flux of ~ 70 – $90\text{ Gg CHBr}_3\text{ yr}^{-1}$.

Estimates of tropical bromoform emissions using an inversion method

M. J. Ashfold et al.

Title Page

Abstract

Introduction

Conclusions

References

Tables

Figures

⏪

⏩

◀

▶

Back

Close

Full Screen / Esc

Printer-friendly Version

Interactive Discussion



Estimates of tropical bromoform emissions using an inversion method

M. J. Ashfold et al.

Title Page

Abstract

Introduction

Conclusions

References

Tables

Figures

⏪

⏩

◀

▶

Back

Close

Full Screen / Esc

Printer-friendly Version

Interactive Discussion

Hossaini et al. (2013) have recently compared the impact of including these other four estimates in the same global model, and found that no single inventory allows a satisfactory match with observations in all locations. The paucity of tropical data, added to the fact that these different studies have used different subsets of those data to construct their inventories, is likely to be one cause of the differing tropical emission values. Overall, the study of Hossaini et al. (2013) supports our finding, that using CHBr_3 measurements from a relatively small number of locations makes constructing (or evaluating) a global emission inventory extremely difficult.

Our estimated emission distributions suggest that coastal CHBr_3 sources, presumably related to seaweed, contribute only a minor fraction of the total tropical emission. We certainly believe that our observations from Tawau were affected by strong, nearby coastal CHBr_3 emissions, but the typical width of the coastal band that is affected by such sources is still not clear (see also Carpenter et al., 2009). The average CHBr_3 mixing ratios we observed inland were lower than at the coast, and we also saw no elevated mixing ratios (i.e. > 5 ppt) inland. This observed gradient occurs over a distance of ~ 50 km, which is well within a typical global model grid cell. The recent study of Leedham et al. (2013), which also focussed on the Maritime Continent, also suggests that the band of coastline directly influenced by macroalgae is likely to be rather narrow. Further investigation of this type of gradient should be a priority because the global impact of coastal emissions is still poorly understood, and the best way to represent them in coarse global models is, therefore, still not clear. This is especially relevant for the Maritime Continent; it is conceivable that much of this region is influenced by coastal processes in some way.

Our examination of the “fine” grid cells near Borneo suggests a moderate (~ 20 %) difference between the emissions that are most suitable for p-TOMCAT (see Fig. 5) and for NAME (i.e. our inversion solutions, Fig. 6). In comparison, the study of Pyle et al. (2011) reported differences of up to a factor of three in the CHBr_3 emissions inferred using these two models, and for a similar area of the Maritime Continent. This may in part be because here we utilise year-round measurements, whereas Pyle et al.

Estimates of tropical bromoform emissions using an inversion method

M. J. Ashfold et al.

Title Page

Abstract

Introduction

Conclusions

References

Tables

Figures

⏪

⏩

◀

▶

Back

Close

Full Screen / Esc

Printer-friendly Version

Interactive Discussion

(2011) considered only a short period in which only southeasterly flow was sampled. Another important difference is that this study uses coastal data, with higher average CHBr_3 mixing ratios, as a constraint. In contrast the p-TOMCAT emissions reported by Pyle et al. (2011), and used here to generate our pseudo observations (Sect. 4), were constrained only by data collected inland at Bukit Atur. Further, those CHBr_3 mixing ratios observed at Bukit Atur in mid-2008 have a mean of 1.21 ppt, which is substantially lower than the long-term (2008–2010) mean of 1.55 ppt for the dataset employed here.

We expect that underlying differences in the efficiency with which these models mix air (i.e. emissions) out of the boundary layer remain an important uncertainty in our emission estimates (see also Robinson et al., 2012). The size of such systematic uncertainties could be explored by using meteorological information from a different forecast centre to drive the NAME dispersion calculations (see Manning et al., 2011, who performed such a test and found little difference in mid-latitudes) and by using a different dispersion model, containing different, or additional parameterisations. Further studies assessing the characteristics of turbulence and related tracer distributions in and immediately above the tropical boundary layer, the influence of small-scale “sea breeze” type circulations, and the representation of these processes in dispersion models, are certainly required.

The limited constraint our new data provide on regional CHBr_3 emissions argues for an expanded network of measurement locations in the Maritime Continent. The spacing of such a network should be similar to the size of the footprint region described here. Further, our two current measurement locations appear to be too close to distinguish between different regional scale influences on air mass composition. This is illustrated by the very similar patterns of variability in our observations of tetrachloroethene (C_2Cl_4), which appears to have few local sources (see Robinson et al., 2013). In addition, the coastal observations used in this study are probably too close to strong CHBr_3 sources to be used to estimate regional-scale emissions. When we attempted to remove the data most influenced by very local emissions we obtained an improved

Estimates of tropical bromoform emissions using an inversion method

M. J. Ashfold et al.

[Title Page](#)[Abstract](#)[Introduction](#)[Conclusions](#)[References](#)[Tables](#)[Figures](#)[⏪](#)[⏩](#)[◀](#)[▶](#)[Back](#)[Close](#)[Full Screen / Esc](#)[Printer-friendly Version](#)[Interactive Discussion](#)

- Carpenter, L. J. and Liss, P. S.: On temperate sources of bromoform and other reactive organic bromine gases, *J. Geophys. Res.-Atmos.*, 105, 20539–20547, doi:10.1029/2000JD900242, 2000. 20465, 20467
- 5 Carpenter, L. J., Jones, C. E., Dunk, R. M., Hornsby, K. E., and Woeltjen, J.: Air-sea fluxes of biogenic bromine from the tropical and North Atlantic Ocean, *Atmos. Chem. Phys.*, 9, 1805–1816, doi:10.5194/acp-9-1805-2009, 2009. 20482, 20484
- Dvortsov, V. L., Geller, M. A., Solomon, S., Schauffler, S. M., Atlas, E. L., and Blake, D. R.: Rethinking reactive halogen budgets in the midlatitude lower stratosphere, *Geophys. Res. Lett.*, 26, 1699–1702, doi:10.1029/1999GL900309, 1999. 20465
- 10 Gostlow, B., Robinson, A. D., Harris, N. R. P., O'Brien, L. M., Oram, D. E., Mills, G. P., Newton, H. M., Yong, S. E., and A Pyle, J.: micro-Dirac: an autonomous instrument for halocarbon measurements, *Atmos. Meas. Tech.*, 3, 507–521, doi:10.5194/amt-3-507-2010, 2010. 20467
- Gschwend, P. M., Macfarlane, J. K., and Newman, K. A.: Volatile halogenated organic-compounds released to seawater from temperate marine macroalgae, *Science*, 227, 1033–1035, doi:10.1126/science.227.4690.1033, 1985. 20465
- 15 Hosking, J. S., Russo, M. R., Braesicke, P., and Pyle, J. A.: Modelling deep convection and its impacts on the tropical tropopause layer, *Atmos. Chem. Phys.*, 10, 11175–11188, doi:10.5194/acp-10-11175-2010, 2010. 20466
- Hossaini, R., Chipperfield, M. P., Monge-Sanz, B. M., Richards, N. A. D., Atlas, E., and Blake, D. R.: Bromoform and dibromomethane in the tropics: a 3-D model study of chemistry and transport, *Atmos. Chem. Phys.*, 10, 719–735, doi:10.5194/acp-10-719-2010, 2010. 20466, 20469
- 20 Hossaini, R., Chipperfield, M. P., Feng, W., Breider, T. J., Atlas, E., Montzka, S. A., Miller, B. R., Moore, F., and Elkins, J.: The contribution of natural and anthropogenic very short-lived species to stratospheric bromine, *Atmos. Chem. Phys.*, 12, 371–380, doi:10.5194/acp-12-371-2012, 2012. 20465
- 25 Hossaini, R., Mantle, H., Chipperfield, M. P., Montzka, S. A., Hamer, P., Ziska, F., Quack, B., Krüger, K., Tegtmeier, S., Atlas, E., Sala, S., Engel, A., Bönisch, H., Keber, T., Oram, D., Mills, G., Ordóñez, C., Saiz-Lopez, A., Warwick, N., Liang, Q., Feng, W., Moore, F., Miller, B. R., Marécal, V., Richards, N. A. D., Dorf, M., and Pfeilsticker, K.: Evaluating global emission inventories of biogenic bromocarbons, *Atmos. Chem. Phys. Discuss.*, 13, 12485–12539, doi:10.5194/acpd-13-12485-2013, 2013. 20483, 20484
- 30

Estimates of tropical bromoform emissions using an inversion method

M. J. Ashfold et al.

Title Page

Abstract

Introduction

Conclusions

References

Tables

Figures

◀

▶

◀

▶

Back

Close

Full Screen / Esc

Printer-friendly Version

Interactive Discussion

Itoh, N. and Shinya, M.: Seasonal evolution of bromomethanes from coralline algae (*Corallinaceae*) and its effect on atmospheric ozone, *Mar. Chem.*, 45, 95–103, doi:10.1016/0304-4203(94)90094-9, 1994. 20465

Jones, A., Thomson, D., Hort, M., and Devenish, B.: The UK Met Office's next-generation atmospheric dispersion model, NAME III, in: *Air Pollution Modeling and Its Application XVII*, edited by: Borrego, C. and Norman, A.-L., Springer US, 580–589, doi:10.1007/978-0-387-68854-1_62, 2007. 20469

Jones, C. E., Andrews, S. J., Carpenter, L. J., Hogan, C., Hopkins, F. E., Laube, J. C., Robinson, A. D., Spain, T. G., Archer, S. D., Harris, N. R. P., Nightingale, P. D., O'Doherty, S. J., Oram, D. E., Pyle, J. A., Butler, J. H., and Hall, B. D.: Results from the first national UK inter-laboratory calibration for very short-lived halocarbons, *Atmos. Meas. Tech.*, 4, 865–874, doi:10.5194/amt-4-865-2011, 2011. 20468

Kirkpatrick, S., Gelatt, C. D., and Vecchi, M. P.: Optimization by simulated annealing, *Science*, 220, 671–680, doi:10.1126/science.220.4598.671, 1983. 20475

Leedham, E. C., Hughes, C., Keng, F. S. L., Phang, S.-M., Malin, G., and Sturges, W. T.: Emission of atmospherically significant halocarbons by naturally occurring and farmed tropical macroalgae, *Biogeosciences*, 10, 3615–3633, doi:10.5194/bg-10-3615-2013, 2013. 20484

Levine, J. G., Braesicke, P., Harris, N. R. P., Savage, N. H., and Pyle, J. A.: Pathways and timescales for troposphere-to-stratosphere transport via the tropical tropopause layer and their relevance for very short lived substances, *J. Geophys. Res.-Atmos.*, 112, D04308, doi:10.1029/2005JD006940, 2007. 20466

Liang, Q., Stolarski, R. S., Kawa, S. R., Nielsen, J. E., Douglass, A. R., Rodriguez, J. M., Blake, D. R., Atlas, E. L., and Ott, L. E.: Finding the missing stratospheric Br_y: a global modeling study of CHBr₃ and CH₂Br₂, *Atmos. Chem. Phys.*, 10, 2269–2286, doi:10.5194/acp-10-2269-2010, 2010. 20465, 20466, 20469, 20483

Manley, S. L., Goodwin, K., and North, W. J.: Laboratory production of bromoform, methylene bromide, and methyl iodide by macroalgae and distribution in nearshore southern California waters, *Limnol. Oceanogr.*, 37, 1652–1659, 1992. 20465

Manning, A. J.: The challenge of estimating regional trace gas emissions from atmospheric observations, *Philos. T. R. Soc. A*, 369, 1943–1954, doi:10.1098/rsta.2010.0321, 2011. 20475

Manning, A. J., Ryall, D. B., Derwent, R. G., Simmonds, P. G., and O'Doherty, S.: Estimating European emissions of ozone-depleting and greenhouse gases using observa-

Estimates of tropical bromoform emissions using an inversion method

M. J. Ashfold et al.

Title Page

Abstract

Introduction

Conclusions

References

Tables

Figures

⏪

⏩

◀

▶

Back

Close

Full Screen / Esc

Printer-friendly Version

Interactive Discussion

tions and a modeling back-attribution technique, *J. Geophys. Res.-Atmos.*, 108, 4405, doi:10.1029/2002JD002312, 2003. 20466, 20471

Manning, A. J., O'Doherty, S., Jones, A. R., Simmonds, P. G., and Derwent, R. G.: Estimating UK methane and nitrous oxide emissions from 1990 to 2007 using an inversion modeling approach, *J. Geophys. Res.*, 116, D02305, doi:10.1029/2010JD014763, 2011. 20466, 20469, 20470, 20471, 20474, 20475, 20476, 20485

Montzka, S. A. and Reimann, S.: Ozone-Depleting Substances (ODSs) and Related Chemicals, vol. Scientific Assessment of Ozone Depletion: 2010, Global Ozone Research and Monitoring Project – Report No. 52, chap. 1, World Meteorological Organization (WMO), Geneva, 2011. 20465, 20467

Moore, R. M., Webb, M., Tokarczyk, R., and Wever, R.: Bromoperoxidase and iodoperoxidase enzymes and production of halogenated methanes in marine diatom cultures, *J. Geophys. Res.-Oceans*, 101, 20899–20908, doi:10.1029/96JC01248, 1996. 20465

Morrison, N. L. and Webster, H. N.: An assessment of turbulence profiles in rural and urban environments using local measurements and numerical weather prediction results, *Bound.-Layer Meteorol.*, 115, 223–239, doi:10.1007/s10546-004-4422-8, 2005. 20469

O'Doherty, S., Cunnold, D. M., Manning, A., Miller, B. R., Wang, R. H. J., Krummel, P. B., Fraser, P. J., Simmonds, P. G., McCulloch, A., Weiss, R. F., Salameh, P., Porter, L. W., Prinn, R. G., Huang, J., Sturrock, G., Ryall, D., Derwent, R. G., and Montzka, S. A.: Rapid growth of hydrofluorocarbon 134a and hydrochlorofluorocarbons 141b, 142b, and 22 from Advanced Global Atmospheric Gases Experiment (AGAGE) observations at Cape Grim, Tasmania, and Mace Head, Ireland, *J. Geophys. Res.*, 109, D06310, doi:10.1029/2003JD004277, 2004. 20466

Ordóñez, C., Lamarque, J.-F., Tilmes, S., Kinnison, D. E., Atlas, E. L., Blake, D. R., Sousa Santos, G., Brasseur, G., and Saiz-Lopez, A.: Bromine and iodine chemistry in a global chemistry-climate model: description and evaluation of very short-lived oceanic sources, *Atmos. Chem. Phys.*, 12, 1423–1447, doi:10.5194/acp-12-1423-2012, 2012. 20465, 20466, 20483

Palmer, C. J. and Reason, C. J.: Relationships of surface bromoform concentrations with mixed layer depth and salinity in the tropical oceans, *Global Biogeochem. Cy.*, 23, GB2014, doi:10.1029/2008GB003338, 2009. 20466

Parrella, J. P., Jacob, D. J., Liang, Q., Zhang, Y., Mickley, L. J., Miller, B., Evans, M. J., Yang, X., Pyle, J. A., Theys, N., and Van Roozendael, M.: Tropospheric bromine chemistry: implica-

Estimates of tropical bromoform emissions using an inversion method

M. J. Ashfold et al.

Title Page

Abstract

Introduction

Conclusions

References

Tables

Figures

⏪

⏩

◀

▶

Back

Close

Full Screen / Esc

Printer-friendly Version

Interactive Discussion

tions for present and pre-industrial ozone and mercury, *Atmos. Chem. Phys.*, 12, 6723–6740, doi:10.5194/acp-12-6723-2012, 2012. 20464

Pike, R. C., Lee, J. D., Young, P. J., Carver, G. D., Yang, X., Warwick, N., Moller, S., Misztal, P., Langford, B., Stewart, D., Reeves, C. E., Hewitt, C. N., and Pyle, J. A.: NO_x and O₃ above a tropical rainforest: an analysis with a global and box model, *Atmos. Chem. Phys.*, 10, 10607–10620, doi:10.5194/acp-10-10607-2010, 2010. 20470

Pisso, I., Haynes, P. H., and Law, K. S.: Emission location dependent ozone depletion potentials for very short-lived halogenated species, *Atmos. Chem. Phys.*, 10, 12025–12036, doi:10.5194/acp-10-12025-2010, 2010. 20466

Polson, D., Fowler, D., Nemitz, E., Skiba, U., McDonald, A., Famulari, D., Marco, C. D., Simmons, I., Weston, K., Purvis, R., Coe, H., Manning, A., Webster, H., Harrison, M., O'Sullivan, D., Reeves, C., and Oram, D.: Estimation of spatial apportionment of greenhouse gas emissions for the UK using boundary layer measurements and inverse modelling technique, *Atmos. Environ.*, 45, 1042–1049, doi:10.1016/j.atmosenv.2010.10.011, 2011. 20466

Press, W. H., Teukolsky, S. A., Vetterling, W. T., and Flannery, B. P.: *Numerical Recipes: The Art of Scientific Computing*, Cambridge University Press, 1986. 20475

Pyle, J. A., Ashfold, M. J., Harris, N. R. P., Robinson, A. D., Warwick, N. J., Carver, G. D., Gostlow, B., O'Brien, L. M., Manning, A. J., Phang, S. M., Yong, S. E., Leong, K. P., Ung, E. H., and Ong, S.: Bromoform in the tropical boundary layer of the Maritime Continent during OP3, *Atmos. Chem. Phys.*, 11, 529–542, doi:10.5194/acp-11-529-2011, 2011. 20466, 20467, 20470, 20473, 20476, 20477, 20479, 20483, 20484, 20485, 20500

Qian, J.-H., Robertson, A. W., and Moron, V.: Diurnal cycle in different weather regimes and rainfall variability over Borneo associated with ENSO, *J. Climate*, 26, 1772–1790, doi:10.1175/JCLI-D-12-00178.1, 2013. 20470

Quack, B. and Suess, E.: Volatile halogenated hydrocarbons over the western Pacific between 43° and 4° N, *J. Geophys. Res.-Atmos.*, 104, 1663–1678, doi:10.1029/98JD02730, 1999. 20467

Quack, B. and Wallace, D. W. R.: Air-sea flux of bromoform: controls, rates, and implications, *Global Biogeochem. Cy.*, 17, 1023, doi:10.1029/2002GB001890, 2003. 20465

Read, K. A., Mahajan, A. S., Carpenter, L. J., Evans, M. J., Faria, B. V. E., Heard, D. E., Hopkins, J. R., Lee, J. D., Moller, S. J., Lewis, A. C., Mendes, L., McQuaid, J. B., Oetjen, H., Saiz-Lopez, A., Pilling, M. J., and Plane, J. M. C.: Extensive halogen-mediated ozone destruction

Estimates of tropical bromoform emissions using an inversion method

M. J. Ashfold et al.

Title Page

Abstract

Introduction

Conclusions

References

Tables

Figures

◀

▶

◀

▶

Back

Close

Full Screen / Esc

Printer-friendly Version

Interactive Discussion

over the tropical Atlantic Ocean, *Nature*, 453, 1232–1235, doi:10.1038/nature07035, 2008. 20464

Reimann, S., Manning, A. J., Simmonds, P. G., Cunnold, D. M., Wang, R. H. J., Li, J. L., McCulloch, A., Prinn, R. G., Huang, J., Weiss, R. F., Fraser, P. J., O'Doherty, S., Greal-
5 ally, B. R., Stemmler, K., Hill, M., and Folini, D.: Low European methyl chloroform emissions inferred from long-term atmospheric measurements, *Nature*, 433, 506–508, doi:10.1038/nature03220, 2005. 20466

Robinson, A. D., Harris, N. R. P., Ashfold, M. J., Gostlow, B., Warwick, N. J., O'Brien, L. M., Beardmore, E. J., Nadzir, M. S. M., Ong, S., Peng, L. K., Phang, S. M., Samah, A. A., Ung,
10 H. E., Yong, S. E., and Pyle, J. A.: Long term halocarbon observations from a coastal and an inland site in Sabah, Malaysian Borneo, in preparation, 2013. 20466, 20467, 20468, 20485

Robinson, N. H., Allan, J. D., Trembath, J. A., Rosenberg, P. D., Allen, G., and Coe, H.: The lofting of Western Pacific regional aerosol by island thermodynamics as observed around Borneo, *Atmos. Chem. Phys.*, 12, 5963–5983, doi:10.5194/acp-12-5963-2012, 2012. 20485

Salawitch, R. J., Weisenstein, D. K., Kovalenko, L. J., Sioris, C. E., Wennberg, P. O., Chance, K., Ko, M. K. W., and McLinden, C. A.: Sensitivity of ozone to bromine in the lower stratosphere, *Geophys. Res. Lett.*, 32, L05811, doi:10.1029/2004GL021504, 2005. 20464, 20465

Saltzman, E. S., Aydin, M., De Bruyn, W. J., King, D. B., and Yvon-Lewis, S. A.: Methyl bromide in preindustrial air: measurements from an Antarctic ice core, *J. Geophys. Res.-Atmos.*, 109, D05301, doi:10.1029/2003JD004157, 2004. 20465

Stohl, A., Seibert, P., Arduini, J., Eckhardt, S., Fraser, P., Grealley, B. R., Lunder, C., Maione, M., Mühle, J., O'Doherty, S., Prinn, R. G., Reimann, S., Saito, T., Schmidbauer, N., Simmonds, P. G., Vollmer, M. K., Weiss, R. F., and Yokouchi, Y.: An analytical inversion method for determining regional and global emissions of greenhouse gases: Sensitivity studies and application to halocarbons, *Atmos. Chem. Phys.*, 9, 1597–1620, doi:10.5194/acp-9-1597-2009, 2009. 20474

Sturges, W. T., Cota, G. F., and Buckley, P. T.: Bromoform emission from Arctic ice algae, *Nature*, 358, 660–662, doi:10.1038/358660a0, 1992. 20465

Tokarczyk, R. and Moore, R. M.: Production of volatile organohalogenes by phytoplankton cultures, *Geophys. Res. Lett.*, 21, 285–288, doi:10.1029/94GL00009, 1994. 20465

Wamsley, P. R., Elkins, J. W., Fahey, D. W., Dutton, G. S., Volk, C. M., Myers, R. C., Montzka, S. A., Butler, J. H., Clarke, A. D., Fraser, P. J., Steele, L. P., Lucarelli, M. P., Atlas, E. L., Schauffler, S. M., Blake, D. R., Rowland, F. S., Sturges, W. T., Lee, J. M.,

Estimates of tropical bromoform emissions using an inversion method

M. J. Ashfold et al.

[Title Page](#)[Abstract](#)[Introduction](#)[Conclusions](#)[References](#)[Tables](#)[Figures](#)[⏪](#)[⏩](#)[◀](#)[▶](#)[Back](#)[Close](#)[Full Screen / Esc](#)[Printer-friendly Version](#)[Interactive Discussion](#)

Penkett, S. A., Engel, A., Stimpfle, R. M., Chan, K. R., Weisenstein, D. K., Ko, M. K. W., and Salawitch, R. J.: Distribution of halon-1211 in the upper troposphere and lower stratosphere and the 1994 total bromine budget, *J. Geophys. Res.-Atmos.*, 103, 1513–1526, doi:10.1029/97JD02466, 1998. 20465

5 Warwick, N. J., Pyle, J. A., Carver, G. D., Yang, X., Savage, N. H., O'Connor, F. M., and Cox, R. A.: Global modeling of biogenic bromocarbons, *J. Geophys. Res.-Atmos.*, 111, D24305, doi:10.1029/2006JD007264, 2006. 20465, 20466, 20469, 20476, 20483, 20500

Webster, H. N., Thomson, D. J., and Morrisson, N. L.: New turbulence profiles for NAME, *Turbulence and Diffusion Note No. 288*, 2003. 20469

10 Yang, X., Cox, R. A., Warwick, N. J., Pyle, J. A., Carver, G. D., O'Connor, F. M., and Savage, N. H.: Tropospheric bromine chemistry and its impacts on ozone: a model study, *J. Geophys. Res.-Atmos.*, 110, D23311, doi:10.1029/2005JD006244, 2005. 20464

Yokouchi, Y., Li, H.-J., Machida, T., Aoki, S., and Akimoto, H.: Isoprene in the marine boundary layer (southeast Asian Sea, eastern Indian Ocean, and southern Ocean): comparison with dimethyl sulfide and bromoform, *J. Geophys. Res.*, 104, 8067–8076, doi:10.1029/1998JD100013, 1999. 20467

Yokouchi, Y., Hasebe, F., Fujiwara, M., Takashima, H., Shiotani, M., Nishi, N., Kanaya, Y., Hashimoto, S., Fraser, P., Toom-Saunry, D., Mukai, H., and Nojiri, Y.: Correlations and emission ratios among bromoform, dibromochloromethane, and dibromomethane in the atmosphere, *J. Geophys. Res.-Atmos.*, 110, D23309, doi:10.1029/2005JD006303, 2005. 20465

20 Ziska, F., Quack, B., Abrahamsson, K., Archer, S. D., Atlas, E., Bell, T., Butler, J. H., Carpenter, L. J., Jones, C. E., Harris, N. R. P., Hepach, H., Heumann, K. G., Hughes, C., Kuss, J., Krüger, K., Liss, P., Moore, R. M., Orlikowska, A., Raimund, S., Reeves, C. E., Reifenhäuser, W., Robinson, A. D., Schall, C., Tanhua, T., Tegtmeier, S., Turner, S., Wang, L., Wallace, D., Williams, J., Yamamoto, H., Yvon-Lewis, S., and Yokouchi, Y.: Global sea-to-air flux climatology for bromoform, dibromomethane and methyl iodide, *Atmos. Chem. Phys. Discuss.*, 13, 5601–5648, doi:10.5194/acpd-13-5601-2013, 2013. 20465, 20483

Estimates of tropical bromoform emissions using an inversion method

M. J. Ashfold et al.

Title Page

Abstract

Introduction

Conclusions

References

Tables

Figures

◀

▶

◀

▶

Back

Close

Full Screen / Esc

Printer-friendly Version

Interactive Discussion

Table 1. The area (in m^2) occupied when different maximum solution grid cell sizes (see also Figs. 3 and 4) are considered, and the percentage of the tropics (20°S – 20°N) this area covers. Then, for experiment D, the total emission from the selected grid (E_{grid}), and that emission extrapolated across the tropics (E_{trop}). Emission units are $\text{Gg CHBr}_3 \text{ yr}^{-1}$.

Max. size	Area	% _{trop}	E_{grid}	E_{trop}
1 by 1	1.65×10^{11}	0.09 %	0.17	180
2 by 2	9.94×10^{11}	0.57 %	1.28	225
4 by 4	4.64×10^{12}	2.65 %	6.39	240

Estimates of tropical bromoform emissions using an inversion method

M. J. Ashfold et al.

Title Page

Abstract

Introduction

Conclusions

References

Tables

Figures

◀

▶

◀

▶

Back

Close

Full Screen / Esc

Printer-friendly Version

Interactive Discussion

Table 2. A comparison of the CHBr_3 emission estimates discussed in Sect. 5. Emissions are listed for the “fine” solution grid cells (inside the solid black contour in Fig. 2, and in red/orange in Fig. 3). The grid cell-by-grid cell mean emission magnitude is given, with the range of the 25 separate solutions in parentheses. Emission units are $\text{Gg CHBr}_3 \text{ yr}^{-1}$. The percentage of the total emission from land (La), coast (Co) and ocean (Oc) grid cells is also noted, with surface definitions taken from the UM land/sea mask. Key to experiments: A, inland observations from Bukit Atur only; B, observations from coastal location, Tawau, included too; C, coastal data capped at the 90th percentile; D, as C but land emissions fixed to zero; E, as D, but using a lower baseline mixing ratio of 0.24 ppt; F, as D, but using a higher baseline mixing ratio of 0.62 ppt.

Exp.	Emission	% _{La}	% _{Co}	% _{Oc}	NMSE
A	1.2 (1.3–1.4)	12	16	72	0.24
B	2.2 (2.0–2.3)	23	26	51	1.05
C	1.4 (1.3–1.5)	17	21	62	0.26
D	1.3 (1.1–1.4)	8	25	67	0.26
E	1.5 (1.3–1.6)	9	26	65	0.21
F	1.1 (1.0–1.2)	8	25	67	0.34

Estimates of tropical bromoform emissions using an inversion method

M. J. Ashfold et al.

Table 3. The split between land (La), coast (Co) and ocean (Oc) when maximum grid cells of different sizes are considered. Key to the headings: A – the area occupied by grid cells of a particular surface type, as a percentage of the total area occupied for each maximum grid size (which is given in Table 1); E – for experiment D, the total emission from grid cells of a particular surface type, in Gg CHBr₃ yr⁻¹; F – for experiment D, the area-averaged flux from grid cells of a particular surface type, in ng CHBr₃ m⁻² s⁻¹ (compare with the maximum fluxes noted under each plot in Figs. 5 and 6).

Max. size	A_{La}	E_{La}	F_{La}	A_{Co}	E_{Co}	F_{Co}	A_{Oc}	E_{Oc}	F_{Oc}
1 by 1	34 %	0.00	0.00	34 %	0.07	0.04	31 %	0.10	0.06
2 by 2	32 %	0.10	0.01	22 %	0.32	0.05	45 %	0.86	0.06
4 by 4	19 %	0.99	0.04	15 %	0.71	0.03	67 %	4.69	0.05

Title Page

Abstract

Introduction

Conclusions

References

Tables

Figures

⏪

⏩

◀

▶

Back

Close

Full Screen / Esc

Printer-friendly Version

Interactive Discussion

Estimates of tropical bromoform emissions using an inversion method

M. J. Ashfold et al.

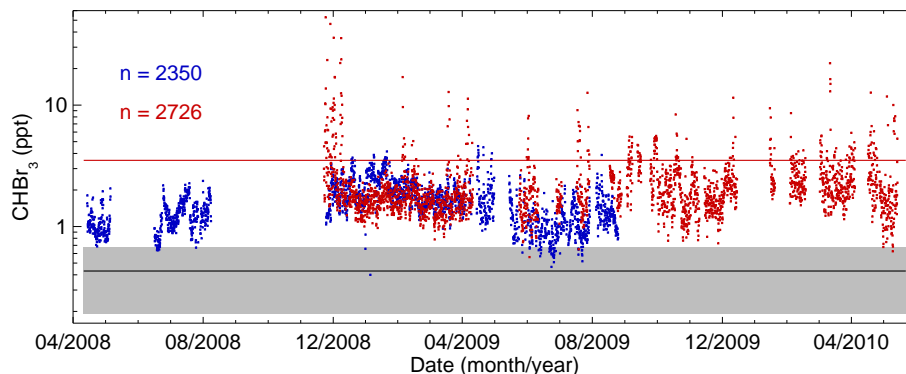


Fig. 1. Observations of CHBr_3 , averaged over 3 h periods, from two locations in northern Borneo for April 2008 to May 2010. The blue data are from Bukit Atur, a rainforest location, and the red data are from Tawau, a coastal site. The solid black line marks the “baseline” mixing ratio of 0.43 ppt assumed in the majority of the inversion experiments (see Sect. 3.2 for details). The shaded grey region indicates one standard deviation (± 0.24 ppt) of the noise added to the observations (or equivalently the baseline, see Sect. 3.2.4). The solid red line, at 3.51 ppt, marks the 90th percentile of the coastal observations. The y-axis is logarithmic. The number of 3 h periods for which observations are available is noted to the top-left of the plot.

[Title Page](#)[Abstract](#)[Introduction](#)[Conclusions](#)[References](#)[Tables](#)[Figures](#)[◀](#)[▶](#)[◀](#)[▶](#)[Back](#)[Close](#)[Full Screen / Esc](#)[Printer-friendly Version](#)[Interactive Discussion](#)

Estimates of tropical bromoform emissions using an inversion method

M. J. Ashfold et al.

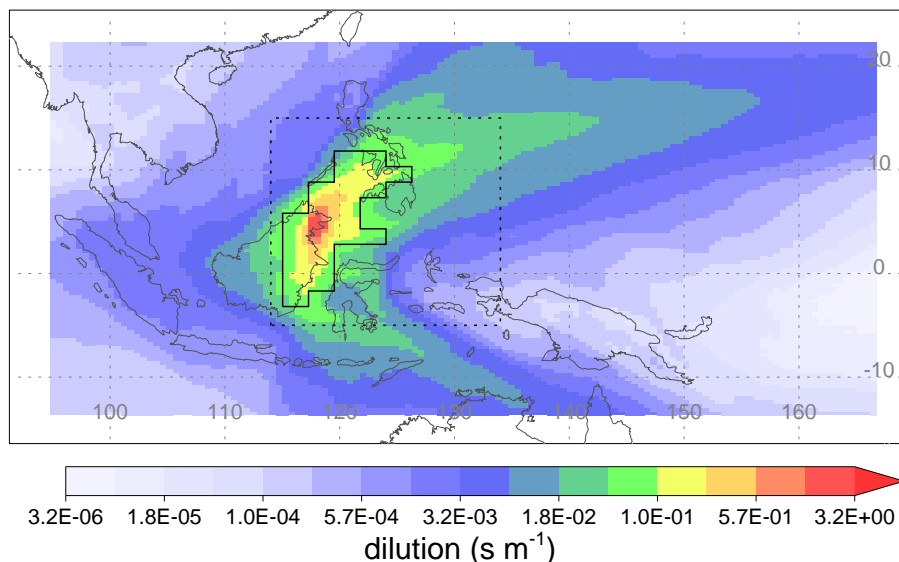


Fig. 2. The mean dilution matrix, averaged over backward trajectories released from both measurement locations, and over all 3 h periods for which observations are available at a particular measurement location. The grid covers $\sim 95\text{--}165^\circ\text{E}$, $13.5^\circ\text{S--}22^\circ\text{N}$ (128 by 96 grid cells). The units are s m^{-1} and the colour scale is logarithmic. The solid black contour encloses the “fine” cells in the solution grid for which emission estimates are subsequently given. The dotted black box highlights the region plotted in Figs. 5 and 6.

Title Page

Abstract

Introduction

Conclusions

References

Tables

Figures

◀

▶

◀

▶

Back

Close

Full Screen / Esc

Printer-friendly Version

Interactive Discussion

Estimates of tropical bromoform emissions using an inversion method

M. J. Ashfold et al.

Title Page

Abstract

Introduction

Conclusions

References

Tables

Figures

◀

▶

◀

▶

Back

Close

Full Screen / Esc

Printer-friendly Version

Interactive Discussion

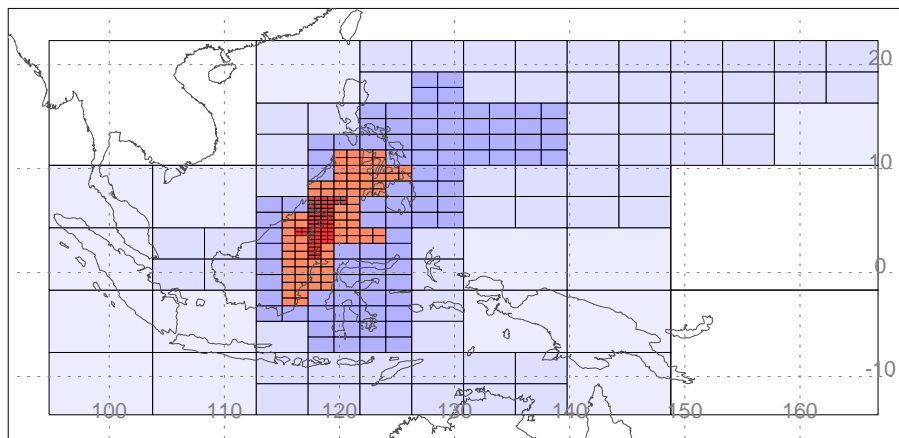


Fig. 3. The solution grid, which contains cells of various sizes, and covers the same area as the dilution grid (Fig. 2). The “fine” grid cells (of size 1 by 1 and 2 by 2 dilution grid cells) are coloured in red/orange.

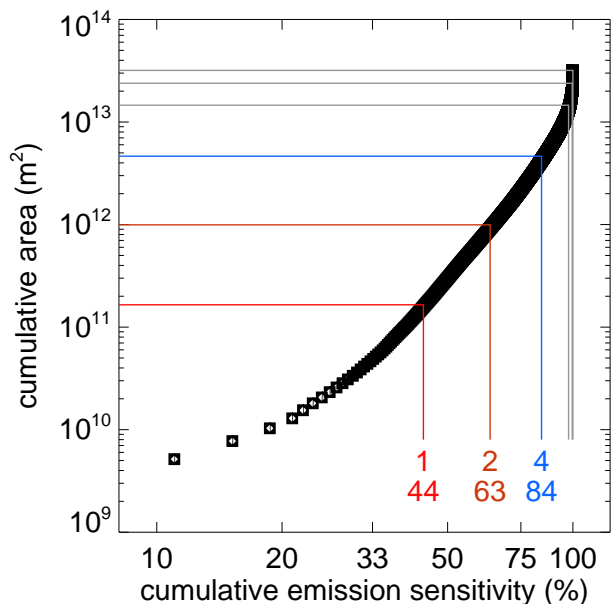


Fig. 4. Each black square represents an individual grid cell in the dilution matrix presented in Fig. 2 and, assuming a uniform emission throughout that area, shows the cumulative percentage of a modelled concentration that is accounted for by adding emissions from that grid cell. The grid cells are counted successively, beginning with the grid cell containing the highest dilution value and finishing with the grid cell containing the lowest. This accumulated percentage is plotted against the surface area covered by the increasing number of grid cells considered. The lines relate to the different sized grid cells in the inversion solution grid. The red line (and label) shows that 44 % of the hypothetical modelled concentration is caused by emissions in grid cells of size 1 by 1, which cover an area of $1.65 \times 10^{11} \text{ m}^2$. The orange (2 by 2), blue (4 by 4) and grey (8 by 8 to 32 by 32) lines indicate this relationship when solution grid cells of increasing size are also included in the calculation. For reference, the surface area between 20° S – 20° N is $1.75 \times 10^{14} \text{ m}^2$.

Estimates of tropical bromoform emissions using an inversion method

M. J. Ashfold et al.

Title Page

Abstract Introduction

Conclusions References

Tables Figures

⏪ ⏩

⏴ ⏵

Back Close

Full Screen / Esc

Printer-friendly Version

Interactive Discussion



Estimates of tropical bromoform emissions using an inversion method

M. J. Ashfold et al.

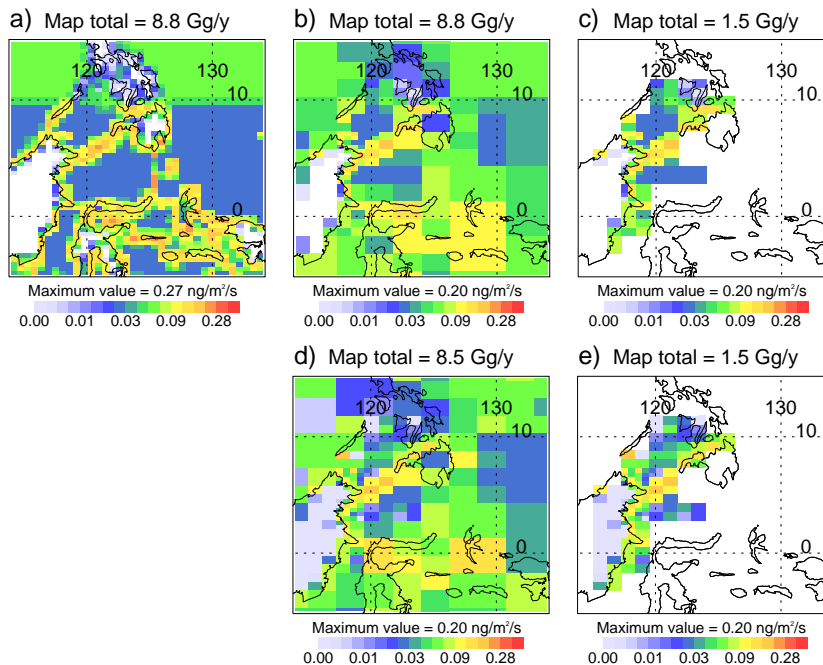


Fig. 5. (a) shows CHBr₃ emissions according to the Pyle et al. (2011) update to scenario 5 in Warwick et al. (2006) after re-gridding to match NAME's grid. These emissions are used to create pseudo observations. (b) shows these emissions degraded to the resolution of the solution grid (see Fig. 3), and (c) shows these degraded emissions when only the "fine" solution grid cells are cut out. For comparison, (d) shows the mean solution of 25 inversions which use pseudo observations derived from the emissions in plot (a), and (e) shows a cut-out of this mean solution for only the "fine" grid cells. The total emission from the plotted grid cells is noted above each plot (units are Gg CHBr₃ yr⁻¹), and the colour scale is exponential.

Estimates of tropical bromoform emissions using an inversion method

M. J. Ashfold et al.

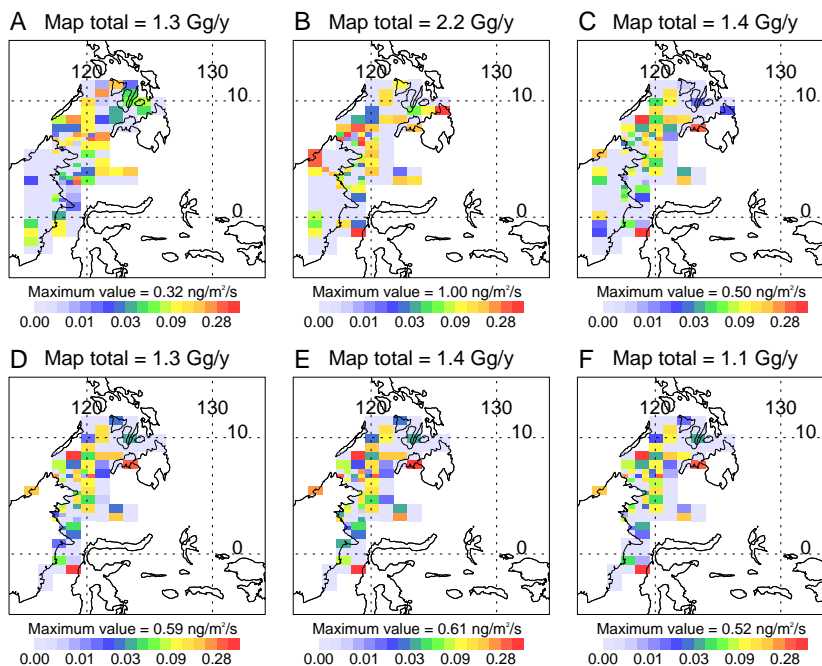


Fig. 6. Estimated emissions of CHBr_3 , for the “fine” grid cells (shades of red in Fig. 3). Experiment labels (see Table 2) are to the top-left of the plots, and in each case the mean of 25 separate solutions to the inversion process is shown. The total emission from the “fine” solution grid cells is noted above the plot (units are $\text{GgCHBr}_3 \text{yr}^{-1}$), and the colour scale is exponential.

Estimates of tropical bromoform emissions using an inversion method

M. J. Ashfold et al.

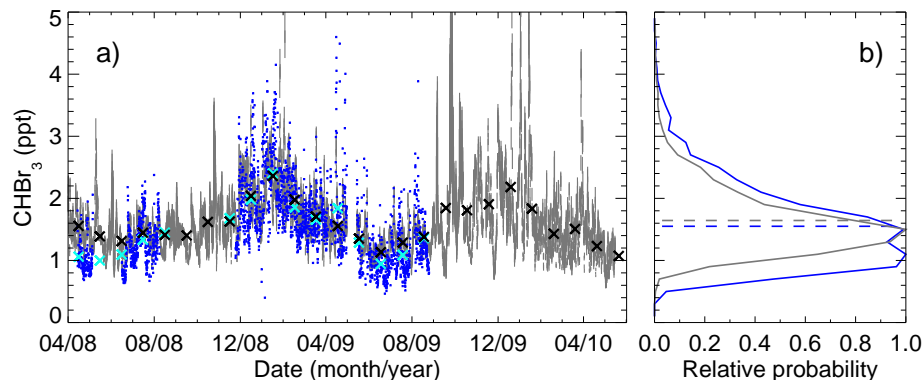


Fig. 7. (a) shows both observed (blue) and modelled (grey) CHBr₃ timeseries at Bukit Atur. The model data are presented as a range, between the smallest and largest mixing ratio simulated in a particular 3 h window using emissions from each of the 25 individual solutions to experiment A. Monthly mean observed (light blue crosses) and modelled (black crosses) mixing ratios are also presented. (b) shows the probability density function for each of these timeseries, normalised using the respective maximum probabilities, and with mean mixing ratios indicated by the dashed lines.

[Title Page](#)[Abstract](#)[Introduction](#)[Conclusions](#)[References](#)[Tables](#)[Figures](#)[◀](#)[▶](#)[◀](#)[▶](#)[Back](#)[Close](#)[Full Screen / Esc](#)[Printer-friendly Version](#)[Interactive Discussion](#)